Influence of Reaction Atmosphere and Heating Rate on *Coffea canephora* husk Pyrolysis for Biochar Production

Bruno F. Coelho,[a] Hérica F. de Almeida,[a] João Gilberto M. Ucella-Filho ,[b] Juliana A. Resende ,[a] Sílvia Cardinal Pinho ,[c] Alina M. Balu ,[d] Edilton N. Silva,[a] Robson C. Sousa ,[a] and Josinaldo de O. Dias [a,*]

Thermochemical conversion of coffee-processing residues into biochar offers a sustainable pathway for biomass valorization, but its properties depend strongly on pyrolysis conditions. This study evaluated how nitrogen and vacuum atmospheres combined with heating rates of 3, 5, and 7 °C min^{-1} affected the yield and physicochemical, structural, and morphological properties of biochar produced from *Coffea canephora* husk at 450 °C. Pyrolysis atmosphere significantly affected biochar yield, averaging 36.5% under nitrogen and 34.1% under vacuum, whereas heating rate had no significant effect within the range investigated. The biochars contained 53.7 to 59.5% fixed carbon and exhibited alkaline pH values from 9.57 to 11.60. True density was significantly influenced by the interaction between atmosphere and heating rate. Structural characterization indicated a reduction in FTIR bands associated with oxygen-containing groups and a predominantly disordered carbonaceous matrix. Qualitative SEM observations suggested a more open surface morphology in biochars produced under vacuum than under nitrogen. These findings indicate that pyrolysis atmosphere influences the properties of coffee husk biochar and support further evaluation of its suitability for agronomic and environmental applications.

DOI: 10.15376/biores.22.1.535-557

Keywords: Char; Thermochemical conversion; Agro-industrial waste; Vacuum pyrolysis; Carbonaceous material

*Contact information: a: Federal University of Espírito Santo, Alto Universitário, s/n, Guararema, Alegre, Espírito Santo 29500-000, Brazil; b: Federal University of Viçosa, Av. P. H. Rolfs, s/n, University Campus, Viçosa, Minas Gerais 36570-900, Brazil; c: University of Porto, Rua Dr. Roberto Frias, 4200-465 Porto, Portugal; d: University of Córdoba, Campus de Rabanales, Marie Curie Building, Ctra. Nacional IV-A, km 396, 14014 Córdoba, Spain; *Corresponding author:Josinaldo.dias@ufes.br*

INTRODUCTION

Brazil has consolidated its position as the world's largest coffee producer, with an estimated production of 66.2 million processed bags for the 2026 crop year (Conab 2026). In this context, Espírito Santo ranks as the second-largest coffee-producing state in Brazil, behind only Minas Gerais, and stands out as the country's leading producer of *Coffea canephora*, with an estimated annual production of approximately 15 million bags (Incaper 2025; Conab 2026). This large-scale production generates substantial volumes of agro-industrial residues, among which coffee husk stands out as a lignocellulosic material with considerable potential for valorization through thermochemical conversion routes (Silva *et al*. 2022).

In this context, pyrolysis represents an efficient route for the conversion of this biomass, promoting its thermal decomposition in the absence of oxygen and generating three main fractions: biochar, bio-oil, and combustible gases (Hughes *et al*. 2014). In contrast, slow pyrolysis operates at lower heating rates, typically below 10 °C × min^{-1}, and with prolonged residence times, thereby maximizing biochar yield (Foong *et al*. 2020). For this reason, slow pyrolysis is the preferred regime when biochar is the primary product of interest and was therefore adopted in the present study. Among these fractions, biochar has attracted growing worldwide interest due to its high fixed carbon content, condensed aromatic structure, and physicochemical properties, which can be favorable for environmental and agronomic applications, such as soil conditioning, carbon sequestration, and contaminant adsorption (Rodriguez *et al*. 2022; Silva *et al*. 2026). The progressive degradation of oxygen-containing and aliphatic groups, together with the formation of more stable aromatic structures, is a well-documented phenomenon during pyrolysis (Hassan *et al*. 2020; Tomczyk *et al*. 2020).

These properties, however, are not constant, but rather result from the interaction between the feedstock and the operational conditions of the process, among which the reaction atmosphere plays a central role in determining the chemical and structural evolution of the material. In systems operated under a nitrogen flow, volatile compounds tend to remain in the reactor for longer periods, favoring secondary condensation reactions and carbon deposition onto the solid matrix (Leng and Huang 2018; Cheng *et al*. 2021). Under vacuum conditions, the more rapid removal of vapors can alter the reaction pathways, thereby affecting the yield, composition, and microstructure of the resulting biochar (Ullah *et al*. 2019; Chmingui *et al*. 2026). The heating rate represents another critical process parameter, governing the kinetics of biomass decomposition and the rate of volatile compound release (Chen *et al*. 2014). Lower heating rates promote gradual devolatilization and greater structural reorganization of the carbonaceous matrix, whereas higher heating rates intensify kinetic effects, thereby influencing carbon retention and the development of the porous structure (Ullah *et al*. 2019; Patra *et al*. 2021).

Although studies have investigated the pyrolysis of coffee husk under isolated conditions (Silva *et al*. 2022; Ninlaphong *et al*. 2025; Chmingui *et al*. 2026), approaches that comprehensively assess the combined effects of the reaction atmosphere and heating rate on the overall physicochemical and structural properties of biochar remain scarce. This gap hinders an integrated understanding of the mechanisms involved and limits the identification of suitable operating conditions for tailoring the material to specific applications. Thus, the present study systematically and comparatively investigates the effects of the pyrolysis atmosphere (nitrogen and vacuum) and three rates of temperature rise on the properties of biochars produced from coffee husk of the species *Coffea canephora*. The materials were characterized by proximate analysis, pH, true density, Fourier-transform infrared spectroscopy (FTIR), X-ray diffraction (XRD), scanning electron microscopy (SEM), and ternary diagram analysis, providing an integrated experimental basis for comparing the resulting biochars and identifying properties relevant to potential environmental and agronomic applications.

EXPERIMENTAL

Thermogravimetric Analysis of Coffee Husk

The raw material used in this study was *Coffea canephora* coffee husk. The initial moisture content of the biomass was 6.27 ± 0.08% on a wet basis. On a dry basis, proximate

analysis yielded 6.33 ± 0.30% ash, 77.49 ± 1.90% volatile matter, and 16.18 ± 2.10% fixed carbon. The biomass also contained, on a dry basis, 27.85 ± 0.08% extractives, 30.55 ± 0.35% insoluble lignin, 3.24 ± 0.03% soluble lignin, and 38.36 ± 0.25% holocellulose. The coffee husk was oven-dried at 105 °C for 24 h, ground, and sieved to obtain particles with diameters ranging from 0.8 to 3.75 mm. The resulting material was subsequently stored until the experiments were conducted.

The thermal stability and degradation behavior of the coffee husk were evaluated by thermogravimetric analysis (TGA) using a TGA/SDTA 851e thermal analyzer (Mettler-Toledo AG, Schwerzenbach, Switzerland) under an inert atmosphere. The analyses were conducted under a continuous nitrogen (N_2) flow at a rate of 50 mL min^{-1} to prevent oxidative reactions during heating. Approximately 4 mg of the previously dried and ground sample were placed in alumina crucibles. The experiments were conducted from room temperature to 900 °C at heating rates of 3, 5, and 7 °C min^{-1}, allowing the influence of the heating rate on the thermal behavior of the material to be evaluated. The variation in heating rate was investigated to assess kinetic effects during the thermal degradation process, including shifts in decomposition temperatures and changes in the intensity of mass-loss peaks.

Pyrolysis Process

A single fixed-bed pyrolysis reactor was operated in two configurations to investigate the effects of the operating atmosphere on biochar formation (Fig. 1). System A operated under a continuous nitrogen flow, whereas System B operated under reduced pressure. Both configurations used the same stainless-steel reactor (120 × 150 × 180 mm), coupled to an electric muffle furnace (ForteLAB, model FCN-1200, 10 L chamber, São Carlos, Brazil) and connected to a refrigerated condensation system. Furnace temperature was controlled by an integrated digital PID controller, while reactor and vapor temperatures were monitored using K-type thermocouples and PT-100 sensors. The vapors passed through condensers connected to an ultrathermostatic bath (Solab, model SL-152, Piracicaba, Brazil) maintained at approximately 12 °C for recovery of the liquid fraction. For each experimental run, 300 g of coffee husk was increased in temperature at a controlled rate of 3, 5, or 7 °C min^{-1} to a final temperature of 450 °C, which was maintained for 60 min. Each combination of pyrolysis atmosphere and heating rate was tested in three independent runs (n = 3), with each run serving as an experimental unit.

System A – Pyrolysis under Nitrogen: Pyrolysis was carried out in a muffle furnace under an inert atmosphere using a continuous nitrogen flow of 0.4 L min^{-1} to ensure oxygen-free conditions.

System B – Vacuum Pyrolysis: Vacuum pyrolysis was conducted under the same thermal conditions and feedstock load, but without gas flow, using a reduced pressure of approximately −200 mmHg. This condition promoted the faster removal of volatile compounds and reduced the vapor residence time within the reactor, directly influencing product distribution and the chemical composition of the biochar and bio-oil.

To ensure experimental organization and traceability, the biochar samples were identified according to the operating conditions employed. Materials produced under a nitrogen atmosphere were designated as PN, whereas those produced under vacuum were designated as PV. Each sample was assigned a numerical suffix corresponding to the heating rate used, with 03, 05, and 07 referring to heating rates of 3, 5, and 7 °C min^{-1}, respectively. Accordingly, the experimental treatments were designated as PN03, PN05, PN07, PV03, PV05, and PV07.

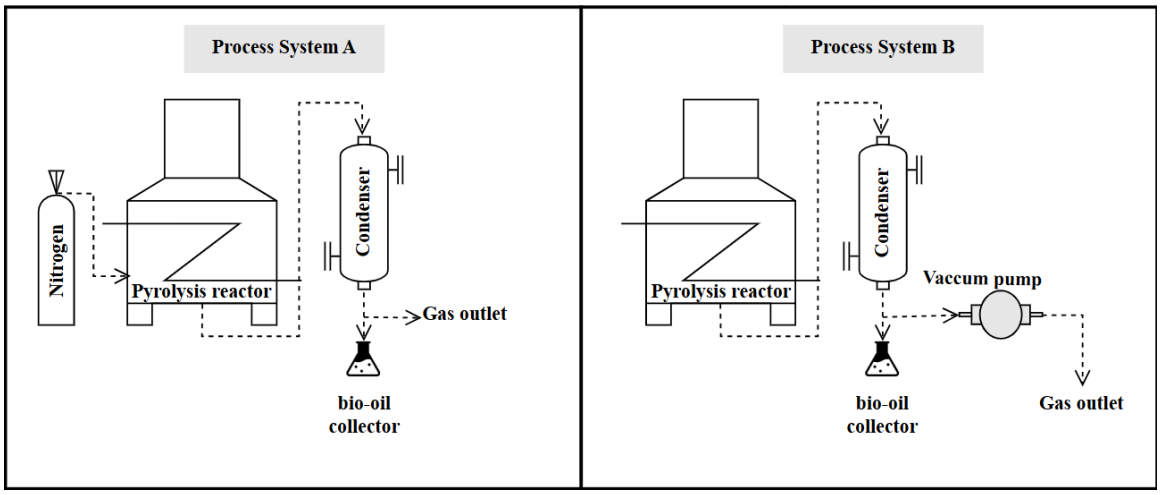


Fig. 1. Experimental apparatus for pyrolysis under nitrogen and vacuum conditions

The gravimetric biochar yields were determined using Eq. 1 to evaluate the efficiency of the pyrolysis process, as follows,

$$Y_{biochar} = \left(\frac{M_{cv}}{M_m}\right) * 100 \quad (1)$$

where $Y_{biochar}$ is the biochar yield (%), M_{cv} is biochar mass (g), and M_m is the dry coffee husk mass (g). The yields of condensable and non-condensable products were not evaluated in this study.

A completely randomized, multilevel 2 × 3 full factorial design was used, combining two reaction atmospheres with three heating rates. The six treatment combinations and their replication are summarized in Table 1. The rates of 3 to 7 °C min^{-1} were selected to compare gradual heating within the slow-pyrolysis regime while keeping final temperature and holding time constant. Nitrogen and vacuum were compared to examine the influence of an inert gas flow versus reduced pressure on volatile removal and biochar formation.

Each run used 300 g of coffee husk; the design comprised 18 independent pyrolysis runs. Nitrogen flow was 0.4 L min^{-1}, and the vacuum configuration operated at approximately −200 mmHg, as described.

Table 1. Experimental Design for Coffee Husk Pyrolysis

Treatment	Atmosphere	Heating rate (°C min^{-1})	Final temperature (°C)	Holding time (min)	Independent runs
PN03	Nitrogen	3	450	60	3
PN05	Nitrogen	5	450	60	3
PN07	Nitrogen	7	450	60	3
PV03	Vacuum	3	450	60	3
PV05	Vacuum	5	450	60	3
PV07	Vacuum	7	450	60	3

Chemical, Functional, and Morphological Characterization of Biochar

Proximate analysis, including moisture, volatile matter, fixed carbon, and ash content, was performed according to the procedures described in ASTM D1762-84 (2021). The biochars were functionally classified by plotting the proximate analysis results on a ternary diagram based on the relative proportions of fixed carbon (FC), volatile matter (VM), and ash (A). Each biochar produced under the different pyrolysis conditions was represented as a point in the diagram, allowing for a comparative visualization of the compositional behavior of the materials. The diagram was interpreted based on functional classification zones defined according to the relative proportions of these three fractions, which distinguish biochars with different levels of stability and functionality and indicate their potential suitability for environmental or agronomic applications.

The environmental potential zone corresponds to biochars with a high fixed carbon content (≥ 50%), low volatile matter content (≤ 30%), and low ash content (≤ 20%), which are characteristics associated with materials exhibiting a higher degree of aromaticity and high chemical stability. The agronomic potential zone is characterized by biochars with moderate to high volatile matter contents (≥ 30%) and fixed carbon contents ≥ 40%, indicating a greater presence of reactive functional groups. The environmental restriction zone is defined by biochars with high ash contents (≥ 70%) and lower proportions of fixed carbon. Finally, the agronomic restriction zone comprises biochars with ash contents ranging from 30% to 70%, volatile matter contents ≥ 30%, and fixed carbon contents ≤ 40%, indicating materials with lower structural stability and limited reactivity, which may restrict their agronomic performance.

The pH was determined in a solid–liquid suspension prepared with distilled water at a ratio of 1:20 (w/v), using a benchtop pH meter (OneSense pH 2500; Marte Científica, Santa Rita do Sapucaí, Brazil). True density was determined using an Ultrapyc 3000 gas pycnometer (Anton Paar, Boynton Beach, FL, USA). Before analysis, the samples were dried at 105 °C and ground. Approximately 5 g of each sample was placed in the measurement cell, and 5.0-grade nitrogen was used as the analysis gas to determine the volume occupied by the sample.

The functional groups of the biochars were characterized by Fourier-transform infrared spectroscopy (FTIR) using a Spectrum 3 spectrometer (PerkinElmer, Waltham, MA, USA) equipped with a MIRacle™ attenuated total reflectance (ATR) accessory with a diamond crystal (PIKE Technologies, Madison, WI, USA). The samples were previously dried and ground and analyzed directly on the ATR crystal without additional chemical preparation. The spectra were acquired over the range of 4000 to 600 cm^{-1} at a resolution of 4 cm^{-1}, with 32 accumulated scans.

The biochars were characterized by X-ray diffraction (XRD) using a MiniFlex diffractometer (Rigaku Corporation, Tokyo, Japan) with Cu Kα radiation (λ = 1.5406 Å), a step size of 0.02°, and a scanning rate of 2° min^{-1}. Before analysis, the samples were dried, ground, and placed in sample holders to obtain a uniform surface. The exported patterns were evaluated over a 2θ range of 10° to 80°. Calcite was identified qualitatively by comparing experimental reflection positions with those calculated from the unit-cell parameters of structure COD 1547350, obtained from the Crystallography Open Database (COD), using Bragg's law and the same wavelength employed in the measurements. The assignment was based on agreement among multiple reflections.

The surface morphology and microstructure of the biochars were evaluated by scanning electron microscopy (SEM) using a JSM-IT200 microscope (JEOL Ltd., Tokyo, Japan) operated under high-vacuum conditions. Before analysis, the samples were dried,

crushed, and mounted on metal stubs using conductive carbon tape. Subsequently, they were sputter-coated with a thin layer of gold to enhance electrical conductivity and minimize charging effects during analysis.

The micrographs were acquired at an accelerating voltage of 10 kV and at different magnifications, enabling a detailed assessment of the surface morphology, pore distribution, and structural characteristics of the material. Image acquisition was performed using a secondary electron (SE) detector to highlight the topographical features of the samples. Qualitative analysis of the micrographs focused on identifying structural changes resulting from the pyrolysis conditions, including pore development, crack formation, and reorganization of the carbonaceous matrix.

Statistical Analysis

The experiment was conducted in a completely randomized full factorial design consisting of two gas-pressure conditions (continuous nitrogen flow and reduced pressure) and three heating rates (3, 5, and 7 °C min^{-1}). Each treatment combination was independently replicated three times (n = 3), with each 300-g pyrolysis batch considered one experimental unit. Statistical analyses were therefore based on independent pyrolysis runs rather than analytical subsamples.

The data obtained were subjected to statistical assumption testing prior to analysis of variance. Residual normality was assessed using the Shapiro–Wilk test, while homogeneity of variances was evaluated using Levene's test, both at a 5% significance level ($p < 0.05$).

When the statistical assumptions were met, the data were subjected to analysis of variance (ANOVA) using a full factorial 2 × 3 design, with pyrolysis atmosphere (nitrogen and vacuum) and heating rate (3, 5, and 7 °C min^{-1}) as the factors. The significance of the main effects and the interaction between the factors was assessed using the F-test at a 5% significance level ($p < 0.05$). When a significant interaction between the factors was observed ($p < 0.05$), comparisons were interpreted for the combinations of atmosphere and heating rate using Tukey's test at the 5% probability level, avoiding the isolated interpretation of the main effects.

Statistical analyses were performed using R software, version 4.4.0 (R Core Team 2024). Graphical representation of the results was performed using the ggplot2 package through boxplots, allowing visualization of data dispersion, medians, and interquartile ranges, together with letters indicating the statistical groupings obtained from Tukey's test.

RESULTS AND DISCUSSION

Thermogravimetric Analysis of Coffee Husk

The coffee husk was subjected to TGA to characterize its thermal decomposition behavior prior to pyrolysis, providing a basis for selecting the final process temperature and evaluating whether the heating rate affects the degradation pattern of the biomass. The TG and DTG curves obtained under an N_2 atmosphere at heating rates of 3, 5, and 7 °C min^{-1} are presented in Fig. 2.

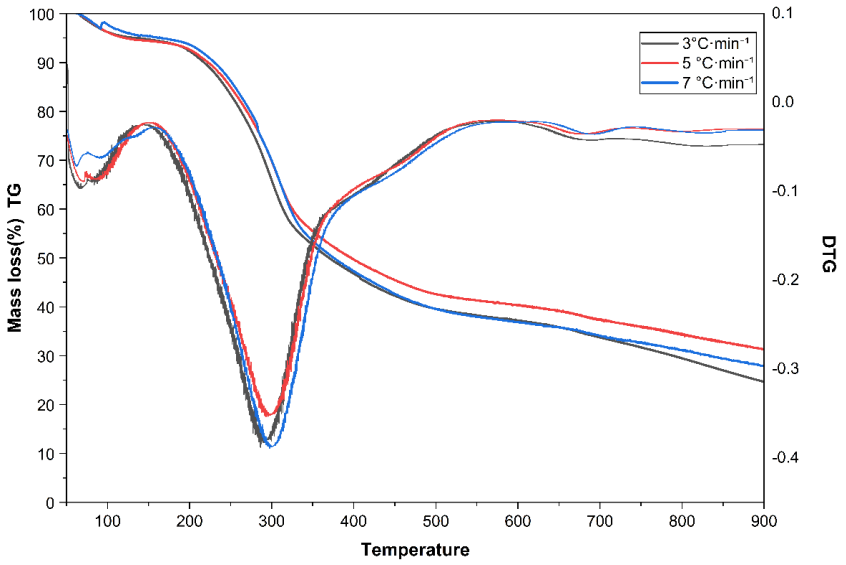


Fig. 2. TG and DTG curves of coffee husk (*Coffea canephora*) obtained under an N_2 atmosphere at different heating rates (3, 5, and 7 °C min^{-1})

The TG and DTG curves obtained at the three heating rates are nearly superimposed, indicating that, within the investigated range, no substantial differences were observed in either the sequence or the temperatures associated with the biomass decomposition stages (Guimarães *et al*. 2020; Radojević *et al*. 2021; Mukherjee *et al*. 2021; Bongomin *et al*. 2025). This finding is relevant because it indicates that the differences subsequently observed in the biochar properties can be attributed primarily to the reaction atmosphere rather than to variations in the intrinsic thermal behavior of the biomass, thereby supporting a direct comparison among the treatments.

The TG curve reveals four characteristic stages of lignocellulosic biomass degradation. The first stage, from 30 to 120 °C, corresponds to the loss of free and surface moisture from the material, observed as a slight initial decrease in the TG curve. From 200 to 280 °C, the DTG curve shows the onset of a more pronounced decline, associated with hemicellulose degradation, a polysaccharide with an amorphous structure and a high proportion of oxygen-containing groups (Radojević *et al*. 2021). In the range of 280 to 350 °C, the most intense peak in the DTG curve was near 300 °C, which is consistent with an important contribution from cellulose decomposition. However, considering that the thermal degradation ranges of hemicellulose, cellulose, and lignin partially overlap, this peak cannot be attributed exclusively to cellulose, nor can it, by itself, be used to conclude that cellulose is responsible for the largest fraction of mass loss.

Above 350 °C, the TG curve shows a progressive decrease in the mass-loss rate up to approximately 900 °C, a behavior attributed to lignin degradation, as lignin is a highly cross-linked aromatic polymer that decomposes over a broad temperature range (Mukherjee *et al*. 2021), favoring the formation of more stable carbonaceous structures that serve as precursors to biochar (Bongomin *et al*. 2025).

The behavior observed in Fig. 2 supports the selection of 450 °C as the final temperature adopted for the pyrolysis process. At this temperature, the main decomposition stages of hemicellulose and cellulose are substantially completed, whereas lignin, due to its greater thermal stability and broad degradation range, remains partially preserved in the solid fraction. A similar behavior was reported by Nguyen *et al*. (2025), who identified the

decomposition of hemicellulose, cellulose, and part of the lignin fraction in coffee husk between 190 and 450 °C, followed by a slower mass loss mainly associated with the degradation of residual lignin and carbonaceous solids. Setter *et al*. (2020) also reported that the main decomposition stage of coffee husk occurs up to approximately 425 °C, whereas above this temperature, the slow degradation of lignin predominates, accompanied by a small additional mass loss. Therefore, a final temperature of 450 °C was selected to ensure the conversion of the more reactive lignocellulosic constituents while partially preserving the carbonaceous structure responsible for biochar formation, as indicated by the TG curve behavior.

Coffee Husk Biochar Yield

Prior to the analysis of variance, the assumptions of residual normality and homogeneity of variances were assessed for all analyzed variables: gravimetric biochar yield, volatile matter, ash and fixed carbon contents, pH, and true density. Residual normality and homogeneity of variances were evaluated using the Shapiro–Wilk and Levene's tests, respectively. For all variables, both tests yielded p-values greater than 0.05, indicating no significant deviations from these assumptions.

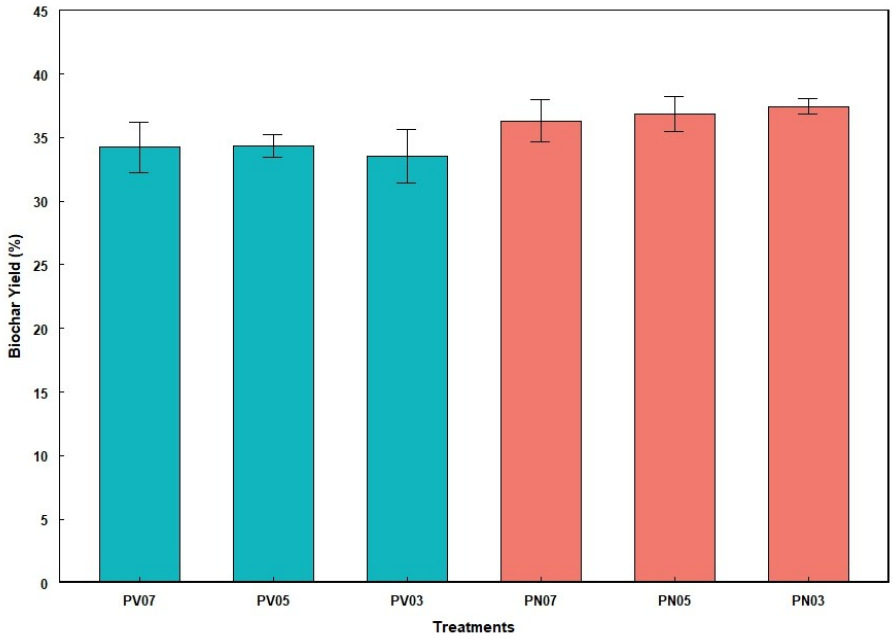


Fig. 3. Gravimetric biochar yield (%) obtained from the pyrolysis of coffee husk (*Coffea canephora*) at 450 °C under nitrogen (PN) and vacuum (PV) atmospheres at heating rates of 3, 5, and 7 °C min^{-1}

The analysis of variance indicated a significant effect only for the pyrolysis atmosphere ($p < 0.05$), with the mean biochar yield being significantly higher under nitrogen (36.5%) than under vacuum (34.1%), as shown in Fig. 3. The heating rate had no significant effect on biochar yield ($p > 0.05$), and no significant interaction between pyrolysis atmosphere and heating rate was observed ($p > 0.05$). Therefore, the main effects were interpreted independently, with the atmosphere being the only factor that significantly influenced the yield of the solid fraction under the evaluated conditions. Saraugi *et al*. (2026), who evaluated heating rates of 2, 6, and 10 °C min^{-1} during the slow pyrolysis of

coconut residues, also found no significant effect of this parameter on biochar yield ($p > 0.05$), indicating that, within the studied range, the pyrolysis temperature had a more pronounced influence on the recovery of the solid fraction.

The absence of an effect of the heating rate is consistent with the thermogravimetric results (Fig. 2). Because the three heating rates produced nearly identical degradation curves, they would likewise be expected to result in no significant differences in the final biochar yield. The difference between the atmospheres, in turn, can be attributed to a single mass-transfer mechanism that manifests differently in each system.

Under a nitrogen atmosphere, the system operates near atmospheric pressure, maintaining a relatively high partial pressure of volatile compounds within the bed. This reduces the concentration gradient between the particles and the surrounding gas phase, thereby slowing the removal of pyrolysis vapors. The resulting longer residence time and prolonged contact of these vapors with the hot char promote secondary reactions and carbon deposition, contributing to the higher biochar yield observed under nitrogen (Zhao *et al*. 2018; Yaashikaa *et al*. 2019; Fu *et al*. 2022; Saraugi *et al*. 2026).

Under vacuum, the reduction in the total system pressure proportionally decreases the partial pressure of the volatiles, increasing the concentration gradient and accelerating their diffusion out of the matrix. With a shorter residence time in the hot zone, these secondary reactions are suppressed, and the fraction that could otherwise be redeposited as solid carbon is removed as vapor, resulting in the lower biochar yield observed under vacuum (Carrier *et al*. 2011; Ullah *et al*. 2019).

Chemical, Functional, and Morphological Characterization of Biochar

Table 2 summarizes the p-values for the effects of pyrolysis atmosphere, heating rate, and their interaction on the quantitative response variables. Although only atmosphere significantly affected biochar yield, significant interactions between atmosphere and heating rate were observed for ash, volatile matter, fixed carbon, pH, and true density. Accordingly, the chemical and physical properties discussed in this section are interpreted considering the combinations of atmosphere and heating rate.

Table 2. ANOVA p Values for the Effects of Atmosphere and Heating Rate

Response variable	Atmosphere	Heating rate	Atmosphere × heating rate
Biochar yield	0.00192	0.23029	0.06850
Moisture	0.00388	3.12×10^{-5}	0.00284
Ash content	0.000531	2.07×10^{-5}	0.000384
Volatile matter	0.168660	4.10×10^{-5}	0.000944
Fixed carbon	0.806005	0.000228	0.013157
pH	3.67×10^{-11}	6.16×10^{-12}	2.15×10^{-11}
True density	$< 2 \times 10^{-16}$	5.24×10^{-15}	3.38×10^{-11}

Significance was assessed at $\alpha = 0.05$. Values are reproduced from Supplementary Tables S1–S6; the full ANOVA tables are retained in the supplementary material.

Effects on Proximate Composition and Ternary Classification

After pyrolysis, all biochars showed a marked reduction in volatile matter and an increase in fixed carbon relative to the precursor biomass (Table 3), demonstrating the effectiveness of the process in removing thermally unstable organic compounds and promoting the formation of a more condensed and aromatic carbon structure (Nanda *et al*. 2016). A similar behavior was reported by Setter *et al*. (2020) for coffee husk pellets subjected to slow pyrolysis within the same temperature range.

Table 3. Proximate Composition of Biochars Produced under Nitrogen and Vacuum at Heating Rates of 3, 5, and 7 °C min^{-1}

Sample	Moisture (%)	Ash (%)	Volatile Matter (%)	Fixed Carbon (%)
PN03	3.81 ± 0.59 b	14.18 ± 0.10 bc	29.40 ± 2.55 b	56.42 ± 2.10 abc
PN05	3.96 ± 0.22 b	13.88 ± 0.35 bc	28.01 ± 0.16 b	58.11 ± 0.26 a
PN07	7.23 ± 0.65 a	13.79 ± 0.13 bc	30.96 ± 0.60 ab	54.84 ± 0.51 bc
PV03	3.39 ± 0.25 b	16.06 ± 0.43 a	24.45 ± 0.49 c	59.50 ± 0.90 a
PV05	4.12 ± 0.69 b	14.54 ± 0.40 b	28.61 ± 1.00 b	56.84 ± 0.64 ab
PV07	4.60 ± 0.78 b	13.47 ± 0.28 c	32.79 ± 0.82 a	53. 74 ± 0.50 c

Note: Treatments sharing the same letter are not significantly different from each other (Tukey, $p < 0.05$).

Under nitrogen, PN07 exhibited a significantly higher moisture content than PN03 and PN05 ($p < 0.05$), which did not differ from each other ($p > 0.05$). Under vacuum, moisture contents were statistically similar across the three heating rates ($p > 0.05$). Comparisons between atmospheres revealed a significant difference only at 7 °C min^{-1}, with PN07 exhibiting a higher moisture content (7.23 ± 0.65%) than PV07 (4.60 ± 0.78%) (Table 3). Thus, the increase in moisture content at the highest heating rate was observed only under nitrogen. Although the water initially present in the biomass is removed during pyrolysis, biochar can subsequently take up moisture during cooling, handling, and storage. This uptake depends on pore accessibility and surface affinity for water, both of which are influenced by structural and chemical changes during carbonization (Tomczyk *et al*. 2020). Foong *et al*. (2020) associated increased moisture contents in cassava stem biochars with greater pore development, which could provide additional sites for water retention. This mechanism offers a possible explanation for the higher moisture content of PN07, although its confirmation requires water uptake measurements under controlled exposure conditions.

Regarding the reaction atmosphere, PV03 exhibited the highest ash content and the lowest volatile matter content among all treatments ($p < 0.05$), differing significantly from the other treatments (Table 3). This result is consistent with the mineral concentration effect previously discussed in relation to biochar yield. Because PV03 experienced the greatest proportional loss of volatile organic matter, the inorganic constituents of the biomass, which do not volatilize, remained concentrated in a smaller residual solid fraction, thereby increasing the proportional ash content (Domingues *et al*. 2017). Under a nitrogen atmosphere, the three treatments showed statistically similar volatile matter contents ($p > 0.05$), suggesting that, under this condition, the heating rate did not influence this fraction. Under vacuum, however, PV03 differed significantly from PV05 and PV07 ($p < 0.05$). The lower heating rate (3 °C min^{-1}) kept the biomass at each temperature range for a longer period, allowing the enhanced removal of volatiles under vacuum to become more pronounced under this specific condition. For fixed carbon, the PN05, PV03, and PV05 treatments comprised the highest-performing group, with no statistically significant

differences among them ($p > 0.05$), whereas PN03, PN07, and PV07 showed lower values (Table 3).

Because fixed carbon is determined by difference from volatile matter and ash contents, this grouping directly reflects the treatments with lower residual volatile matter. PV03, which exhibited the highest ash content, also reached a high fixed carbon content because it had the lowest volatile matter content among all treatments, indicating that, in this dataset, the extent of devolatilization was the determining factor for fixed carbon, outweighing the effect of ash content.

The functional classification of the biochars using the ternary diagram, presented in Fig. 4, was based on the fixed carbon, volatile matter, and ash contents obtained from the proximate analysis. All biochars were positioned between the agronomic and environmental potential zones, with none of the evaluated treatments falling within the agronomic or environmental restriction zones. This result is directly related to the moderate ash contents (13.47 to 16.1%), high fixed carbon contents (53.74 to 59.5%), and intermediate volatile matter contents (24.45 to 32.8%) observed in Table 3.

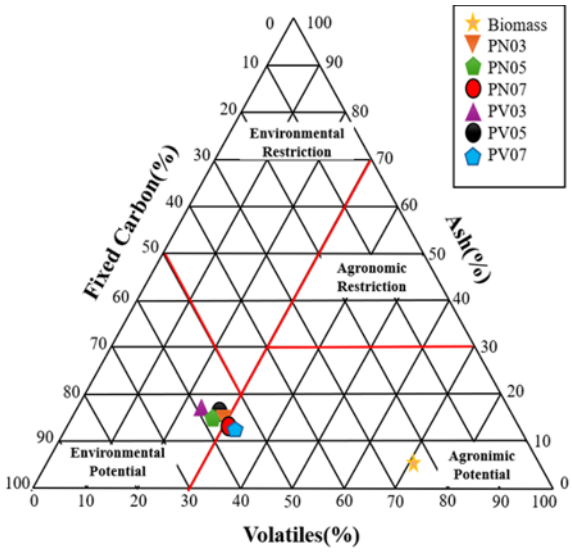


Fig. 4. Classification of biochars produced by pyrolysis of coffee husk using a ternary diagram based on fixed carbon (FC), volatile matter (VM), and ash (A) fractions

The positioning at the boundary between the two potential zones indicates that the biochars produced exhibit characteristics that were simultaneously favorable for chemical stability and surface reactivity, thereby broadening their potential applications. Chmingui *et al*. (2026), who produced biochar by vacuum pyrolysis of olive pomace with a fixed carbon content of 68.7%, estimated a carbon sequestration potential of 2.05 t CO_2eq per ton of biochar, demonstrating the significant climate-mitigation potential of biochars positioned within the environmental potential zone. Although this fixed carbon content is higher than that observed in the present study, it places coffee husk biochars along the same trend toward greater stability.

The PV03 treatment was positioned closer to the environmental potential zone due to its lower volatile matter content (24.5%) among all treatments evaluated (Table 3), a criterion that characterizes this zone according to Rodriguez *et al*. (2022). This positioning is consistent with the agronomic potential previously discussed for coffee husk biochars by Domingues *et al*. (2017), who reported that these materials can act as slow-release

potassium fertilizers due to the high content of this nutrient in the source biomass. This profile is associated with greater chemical stability and resistance to decomposition, characteristics that are favorable for carbon sequestration and environmental remediation (Rodriguez *et al*. 2022).

In contrast, PV07 and PN07 exhibited the highest volatile matter contents, 32.79 ± 0.82% and 30.96 ± 0.60%, respectively, positioning them closer to the agronomic potential zone. According to the classification criteria proposed by Silva *et al*. (2026), this condition is associated with a higher fraction of reactive carbon and greater potential for nutrient availability in the soil. It should be emphasized that volatile matter content alone does not demonstrate nutrient availability or agronomic performance, neither of which was measured in this study.

This distribution among the zones directly reflects the interaction between pyrolysis atmosphere and heating rate during the devolatilization process. Under vacuum, the pressure gradient between the reactor and the vacuum pump causes the released volatiles to diffuse immediately out of the solid matrix, reducing vapor recondensation on the surface of the forming biochar (Foong *et al*. 2020).

From a practical perspective, since none of the treatments were positioned within a restriction zone, the heating rate can be considered a fine-tuning parameter for determining the intended application of the resulting biochar, without requiring changes in the pyrolysis atmosphere. The biochar obtained under PV03, which is more recalcitrant and chemically stable, may indicate potential for long-term carbon sequestration and environmental remediation applications, such as contaminant adsorption (Rodriguez *et al*. 2022). In contrast, the biochars obtained under PN07 and PV07, due to their higher retention of volatile matter, are likely to preserve a greater fraction of oxygen-containing surface functional groups, such as carboxylic and phenolic groups, which are associated with higher cation exchange capacity (Tomczyk *et al*. 2020). These characteristics may indicate potential for their use as agricultural soil amendments, as they may favor short-term nutrient availability.

The classification of the biochars in the ternary diagram indicated both agronomic and environmental potential for all treatments. To further assess this potential, pH was considered as a complementary parameter, as it influences the interaction of biochar with soil acidity and nutrient availability. This property results from the balance between the alkaline mineral fraction, composed mainly of carbonates and basic cations (Yuan *et al*. 2011; Ding *et al*. 2014).

Heating conditions may modify both the retention of mineral species and the persistence of these surface functional groups (Ronsse *et al*. 2013). The effects of these factors are examined below based on the results presented in Fig. 5. All treatments exhibited an alkaline character, with pH values ranging from 9.6 to 11.6. Under a nitrogen atmosphere, a progressive and statistically significant decrease in pH was observed with increasing heating rate ($p < 0.05$), indicating that, under N_2, lower heating rates favor greater retention of alkaline species within the solid matrix, possibly due to the lower rate of volatilization of inorganic compounds (Liu *et al*. 2018). This behavior is consistent with the general mechanism governing biochar pH, in which alkalinity results predominantly from the concentration of carbonates and inorganic bases in the mineral fraction as the organic matrix decomposes (Yuan *et al*. 2011; Ding *et al*. 2014).

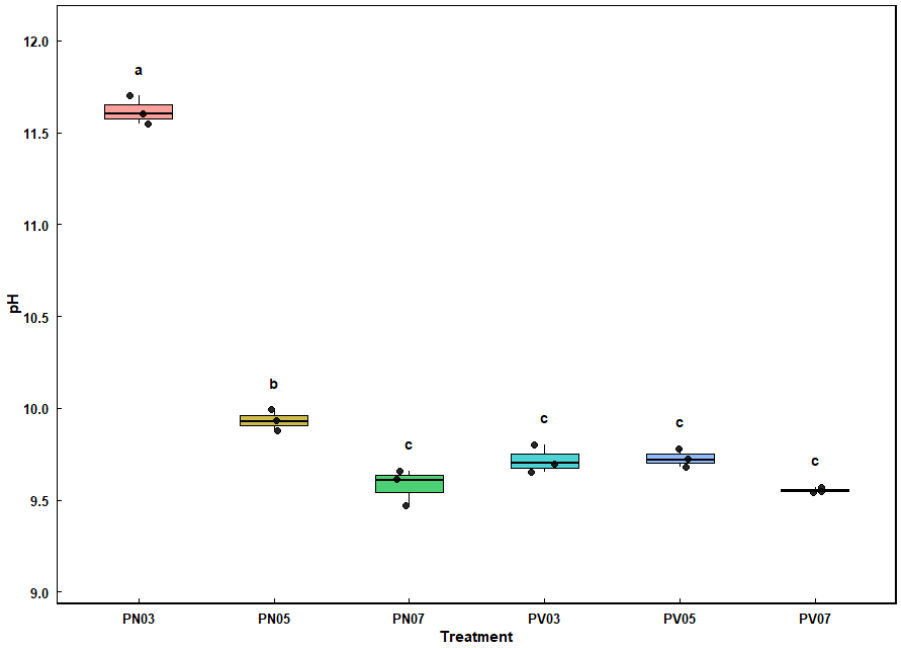


Fig. 5. pH values of biochars produced from coffee husk under nitrogen (PN) and vacuum (PV) atmospheres at different heating rates (3, 5, and 7 °C min^{-1}). Treatments sharing the same letter are not significantly different from each other (Tukey, $p < 0.05$).

Under vacuum, the PV03, PV05, and PV07 treatments did not differ significantly in pH ($p > 0.05$), indicating that reduced pressure suppresses the influence of heating rate on the retention of alkaline compounds. This result is consistent with the mechanism of reduced pressure during vacuum pyrolysis (Panwar and Pawar 2022). Because volatile removal under these conditions is governed primarily by the pressure gradient rather than by the heating rate, the latter becomes less relevant as a control variable for pH under this atmosphere.

Overall, strongly alkaline biochars have been reported in the literature under pyrolysis conditions involving high temperatures, above 600 °C (Nanda *et al*. 2016; Domingues *et al*. 2017; Patra *et al*. 2021). However, in the present study, a high pH was observed for the PN03 sample (11.60 ± 0.01) even under a moderate temperature condition (450 °C), indicating that the combination of a nitrogen atmosphere and a lower heating rate favored the formation of alkaline species without requiring more severe pyrolysis temperatures. This represents an operational and energy advantage for the process.

This advantage further highlights the practical relevance of determining biochar pH, which is a key characterization parameter because it directly influences its intended agronomic application. In acidic soils, alkaline biochars increase soil pH and reduce Al^{3+} toxicity by promoting its precipitation as $Al(OH)_3$ (Shetty *et al*. 2021). Regarding the optimal range for soil application, there is no single value applicable to all contexts, since biochar characterization and selection should be performed according to the intended purpose of application (Pariyar *et al*. 2020).

Highly alkaline biochars, such as PN03, promote faster and more pronounced soil pH correction per unit of applied mass and are therefore suitable for strongly acidic soils. Biochars produced at moderate temperatures, such as those used in the present study (450 °C), are particularly suitable for this corrective function (Shetty *et al*. 2021). However, the use of highly alkaline materials requires careful consideration of the application rate, as

over-liming in soils close to neutrality may induce deficiencies of micronutrients such as iron, manganese, and zinc. In contrast, biochars with pH values closer to neutrality, such as PN07, PV03, PV05, and PV07, provide more gradual pH correction, associated with a longer-lasting complementary effect due to the retention of acidic functional groups.

Thus, the variation in pH among the treatments observed in this study represents, in practical terms, a range of correction intensities and time horizons that can be selected according to the specific requirements of the target soil, further highlighting the agronomic relevance of heating rate as a fine-tuning parameter in this context as well.

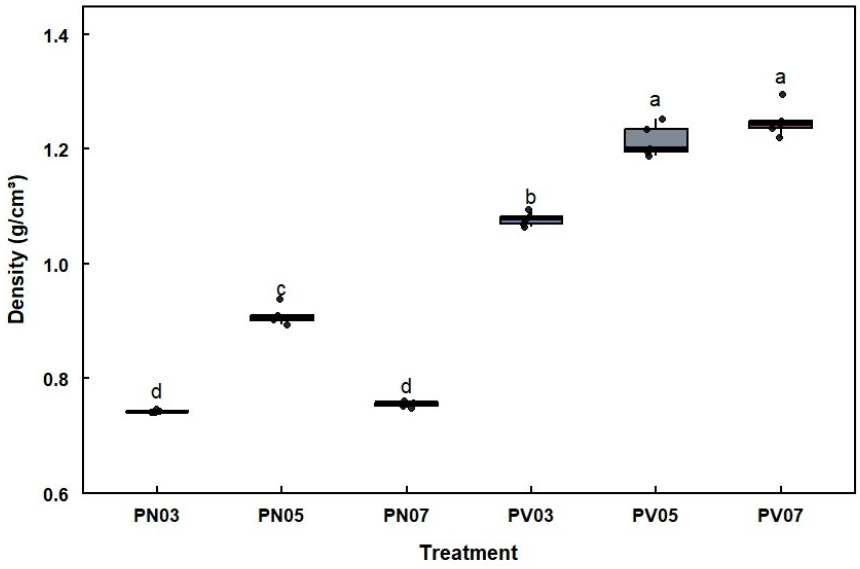


Fig. 6. True density of biochars produced from coffee husk under nitrogen (PN) and vacuum (PV) atmospheres at different heating rates (3, 5, and 7 °C min^{-1}). Treatments sharing the same letter are not significantly different from each other (Tukey, $p < 0.05$).

In addition to the chemical properties represented by pH, biochar application also depends on its physical characteristics. In this context, true density provides information on the organization of the solid matrix and particle composition. The analysis of variance revealed a significant interaction between pyrolysis atmosphere and heating rate for this property ($p < 0.05$), demonstrating that the effect of heating rate varied depending on the atmosphere employed. The results are presented in Fig. 6.

Under a nitrogen atmosphere, PN03 and PN07 exhibited the lowest true density values, whereas PN05 showed a higher value, as observed in the figure above. This non-linear behavior demonstrates that increasing the heating rate did not result in a continuous increase in density under this atmosphere. The PN05 result indicated a more pronounced modification of the solid phase at a heating rate of 5 °C min^{-1}; however, true density alone does not allow this difference to be attributed to structural contraction, as this parameter is also influenced by mineral composition and the presence of pores accessible to the fluid used for its determination.

Under vacuum, true density increased from 3 to 5 °C min^{-1}, a behavior also observed under nitrogen within this range. Overall, the vacuum treatments exhibited higher values than those obtained under N_2. Because a significant interaction between atmosphere and heating rate was observed ($p < 0.05$), the effect of heating rate depended on the atmosphere employed.

The true density values obtained under vacuum (1.073 to 1.247 g cm^{-3}) were higher than those reported by Chmingui *et al*. (2026) for olive pomace biochar produced by vacuum pyrolysis, reinforcing that biomass composition and operating conditions interact to determine the physical properties of the material.

From a practical perspective, lower-density biochars tend to be more advantageous because they can maximize the physical benefits to the soil. In this regard, the nitrogen-produced treatments, which exhibited lower density, may be preferable for this purpose, whereas the denser biochars obtained under vacuum may be more suitable for applications requiring greater structural stability or a lower volume per unit mass.

Functional Groups and Mechanistic Interpretation

The raw biomass exhibited the typical profile of lignocellulosic materials, with a high density of oxygen-containing groups and aliphatic structures, characterized by a broad band between 3600 and 3200 cm^{-1} associated with O–H stretching, bands around 2920 and 2850 cm^{-1} attributed to aliphatic C–H stretching (Liu *et al*. 2018), absorbance in the 1740 to 1700 cm^{-1} region related to carbonyl groups, and a strong contribution in the 1200 to 1000 cm^{-1} region arising from C–O and C–O–C stretching in polysaccharides. This spectral profile confirms a highly functionalized, oxygen-rich matrix with a relatively low degree of condensation and limited thermal stability.

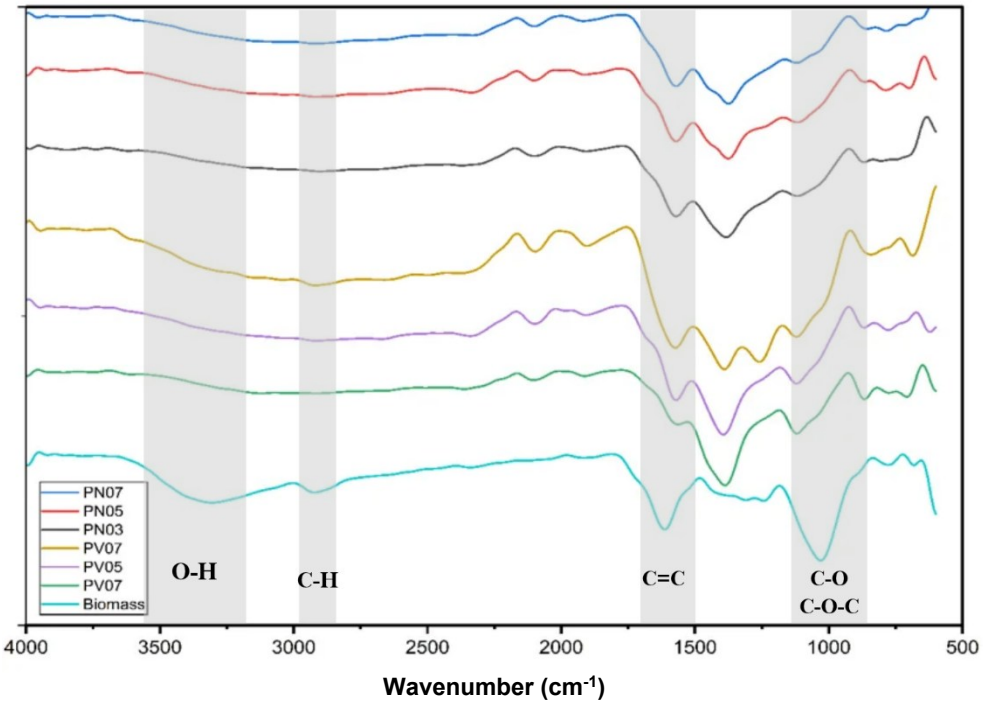


Fig. 7. FTIR spectra of raw coffee husk and biochars in the spectral range of 4000 to 600 cm^{-1}

After pyrolysis, all samples exhibited a reduction in the intensity of bands associated with oxygen-containing groups, accompanied by a relative strengthening of bands attributed to aromatic structures. The relative increase in absorbance in the 1600 to 1500 cm^{-1} region, assigned to aromatic C=C stretching, indicates the reorganization of the solid matrix into polycondensed aromatic domains, which are characteristic of biochars with greater chemical and thermal stability (Domingues *et al*. 2017).

Under a nitrogen atmosphere, the structural evolution of the biochars occurred gradually with increasing heating rate. At 3 °C min^{-1}, the region between 1200 and 1000 cm^{-1} indicates the partial preservation of C–O groups. At a heating rate of 5 °C min^{-1}, these bands became less intense, while the aromatic region became more clearly prominent, indicating an intensification of the reactions. At 7 °C min^{-1} under N_2, a strong suppression of the O–H, C–O, and C=O bands was observed, with predominant absorption around 1580 to 1600 cm^{-1}. This indicates a substantially more aromatized matrix with residual oxygen-containing functional groups, as the inert atmosphere influences secondary recombination reactions among oxygenated fragments, limiting complete deoxygenation (Song *et al*. 2025).

In contrast, the vacuum-produced biochars exhibited a distinct structural evolution, indicating the influence of pressure on the transformation of the material. At 3 °C min^{-1}, the intensity of the bands associated with oxygen-containing groups was lower than that observed under N_2, suggesting that the reduction in the partial pressure of volatiles favors their continuous removal and shifts the system toward more efficient deoxygenation pathways. At the intermediate heating rate of 5 °C min^{-1}, the contribution of the C–O bands became residual, while the aromatic band became predominant in the spectrum, indicating a synergistic effect between heating rate and atmosphere that favors the consolidation of a more stable aromatic matrix (Chmingui *et al*. 2026). At 7 °C min^{-1} under vacuum, the spectrum exhibited the highest degree of functional simplification among all samples analyzed, with an almost exclusive predominance of aromatic bands and a marked absence of detectable oxygen-containing functionalities, evidencing the highest degree of deoxygenation and aromatization achieved in this study.

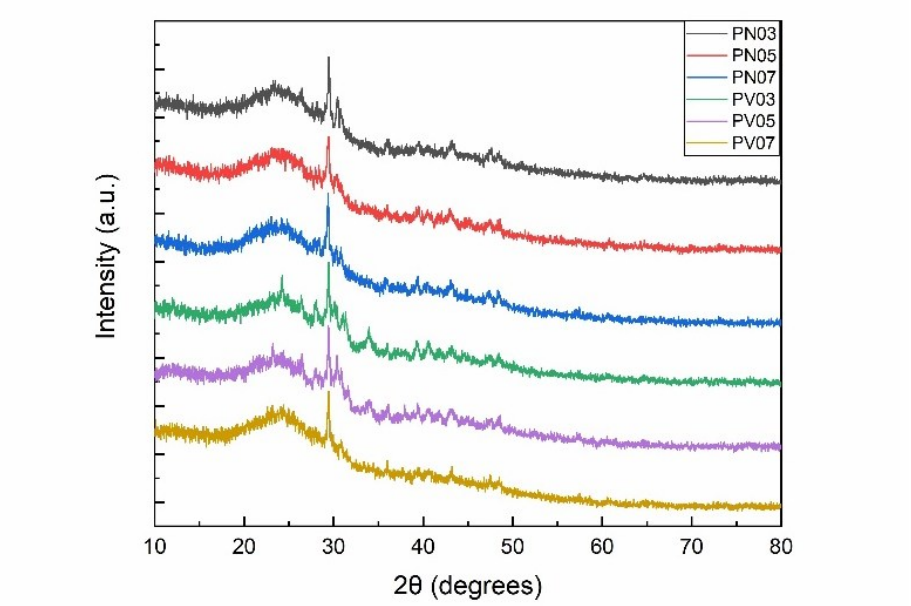


Fig. 8. X-ray diffraction (XRD) patterns of biochars produced from coffee husk under nitrogen (PN) and vacuum (PV) atmospheres at different heating rates (3, 5, and 7 °C min^{-1})

Figure 8 presents the X-ray diffraction patterns of the biochars. All samples exhibited a diffuse contribution in the approximately 20 to 30° 2θ region, superimposed with narrow reflections from crystalline mineral phases. This broad contribution consists of a poorly ordered carbonaceous matrix and with the diffuse scattering associated with turbostratic carbon (Chmingui *et al*. 2026).

The main reflection, located between 29.38° and 29.48°, was consistent with calcite ($CaCO_3$), based on comparison with reference positions calculated from COD 1547350 for Cu Kα radiation (λ = 1.5406 Å). Additional reflections near 36.0°, 39.4°, 43.2°, 47.5°, and 48.5° supported this assignment, although some were poorly resolved in individual samples. Chmingui *et al*. (2026) identified calcite reflections in similar angular regions. The signals between 26° and 27° were left unassigned because comparison with the quartz reference structure did not provide sufficient evidence for identification.

The estimated crystallinity index ranged from 4.7% to 12.3%. Under vacuum, the values decreased with increasing heating rate, from 12.3% for PV03 to 11.9% for PV05 and 4.7% for PV07. Under nitrogen, PN03 exhibited an index of 9.0%, whereas PN05 and PN07 showed similar values of 6.2% and 6.4%, respectively. These comparisons are descriptive, as statistical significance was not assessed. The low indices are consistent with the prominent diffuse contribution observed in the patterns. However, because the integrated crystalline area includes mineral reflections, these values should not be interpreted exclusively as a measure of carbon ordering.

The mineral reflections complement the proximate analysis by identifying crystalline constituents of the inorganic fraction associated with ash, although the crystallinity index is not equivalent to ash content. Calcite may contribute to the alkaline pH of the biochars, consistent with the occurrence of carbonates and other alkaline mineral species reported by Domingues *et al*. (2017). These findings support their potential use in soil acidity management, although their neutralizing capacity requires specific testing.

Effects on Surface Morphology

In addition to the degree of structural ordering identified by XRD, the morphology of the carbonaceous matrix was investigated by scanning electron microscopy (SEM), as presented in Fig. 9. SEM revealed substantial modifications in pore structures, cell wall integrity, and the degree of structural collapse resulting from the release of volatile matter during pyrolysis and the formation of an interconnected porous network (Silva *et al*. 2026). A direct comparison between the samples produced under nitrogen and vacuum atmospheres indicates that the reaction atmosphere played a determining role in the final morphology of the biochar. These images provide qualitative observations of the exposed surfaces and do not quantify total porosity, pore-size distribution, or three-dimensional connectivity. Thus, SEM observations do not establish higher adsorption capacity, water retention, or microbial colonization, all of which require direct testing.

In contrast, the biochars obtained under vacuum exhibited a more open and porous structure, with this behavior becoming more pronounced as the heating rate increased. This behavior is attributed to the reduced pressure, which promotes the immediate release of volatile matter and decreases vapor recondensation on the material surface, resulting in a less obstructed morphology (Foong *et al*. 2020). A more porous structure has been associated in the literature with greater potential for water retention and microbial colonization in soil (Chmingui *et al*. 2026), although quantitative confirmation of this potential for the biochars investigated in this study would require direct determination of the specific surface area (BET), which was not performed in this work. Therefore, the morphological assessment by SEM was treated qualitatively, without inferring specific surface area values.

The influence of heating rate differed depending on the atmosphere employed. Under both atmospheres, the samples obtained at the lowest heating rate exhibited greater preservation of the cell walls, indicating gradual devolatilization and more time available

for structural reorganization of the carbonaceous matrix, a behavior also reported for rapeseed stem biochars produced at different heating rates (Zhao *et al*. 2018). At a heating rate of 5 °C min^{-1}, particularly under vacuum, a more homogeneous microstructure with high pore connectivity was observed, suggesting a balance between the kinetics of thermal decomposition and efficient volatile removal (Ninlaphong *et al*. 2025). At the highest heating rate, particularly under vacuum, irregular pores and partial collapse of the cell walls were observed. In principle, accelerated devolatilization will reduce the time available for structural rearrangement and may thereby intensify the kinetic effects of the process.

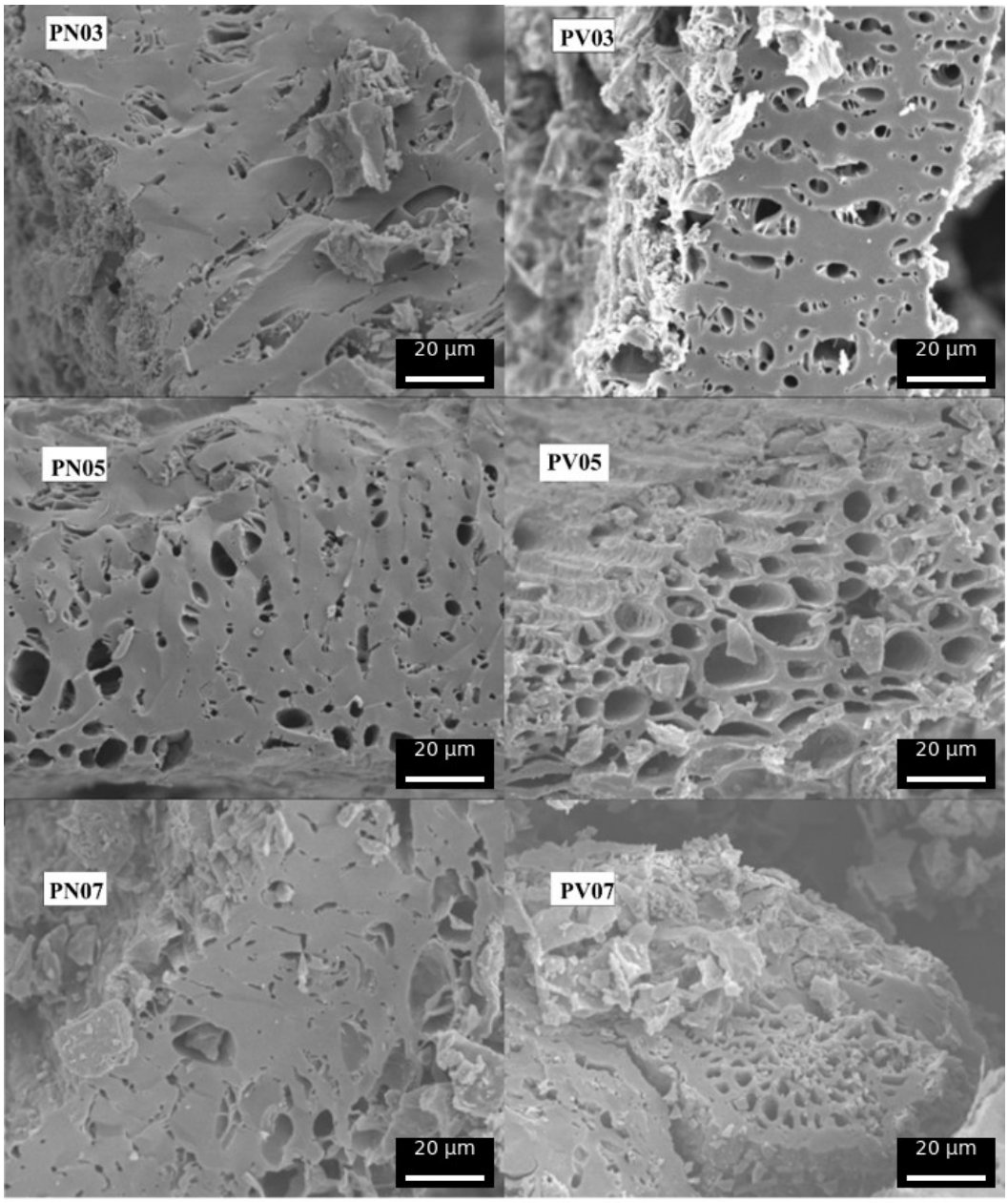


Fig. 9. Scanning electron microscopy (SEM) micrographs of biochars produced from coffee husk under nitrogen (PN) and vacuum (PV) atmospheres at different heating rates (3, 5, and 7 °C min^{-1}), at 1000× magnification

Implications for Biochar Use and Comparison with Coffee Husk Studies

At 450 °C, Domingues *et al*. (2017) reported coffee husk biochar with a yield of 37.7%, 26.2% volatile matter, 12.9% ash, and 60.9% fixed carbon. The present atmosphere-averaged yields were 36.5% under nitrogen and 34.0% under vacuum, with volatile matter of 24.4 to 32.8%, ash of 13.5 to 16.1%, and fixed carbon of 53.7 to 59.5%. These values provide a descriptive comparison, not a statistical test across studies. Differences in feedstock and reactor conditions preclude attributing the contrasts exclusively to atmosphere or heating rate.

Setter *et al*. (2020) investigated the effects of final temperature on coffee husk briquettes, whereas the present work compared atmosphere and heating rate at a fixed final temperature. Its contribution is therefore the factorial comparison of these operating variables at 450 °C rather than the identification of a universally optimal biochar. The alkaline pH and compositional differences indicate treatments for further soil evaluation, while the morphology suggests priorities for quantitative pore characterization.

Application claims remain conditional: soil use requires assessment of neutralizing capacity, salinity, nutrient release, contaminants, and plant response; adsorption requires sorption tests and quantitative surface characterization. No soil, plant, water-retention, adsorption, or carbon-persistence experiment was conducted. The findings are also restricted to one final temperature (450 °C), one holding time (60 min), two operating atmospheres, and heating rates of 3 to 7 °C min^{-1}.

CONCLUSIONS

Within the experimental scope evaluated, the following conclusions can be drawn:

1. Coffee husk demonstrated its feasibility as a precursor for the production of biochars with tunable physicochemical and structural properties.
2. The reaction atmosphere was the main factor governing biochar yield, with nitrogen producing higher yields than vacuum, while the heating rate primarily influenced compositional and structural features rather than overall yield.
3. The combined evidence from proximate analysis, ternary classification, pH, true density, Fourier transform infrared (FTIR), X-ray diffraction (XRD), and scanning electron microscopy (SEM) demonstrated that nitrogen favors more alkaline biochars, whereas vacuum promotes greater deoxygenation and pore development. All treatments remained within agronomic and environmental application zones, with no indication of restrictive characteristics.
4. The results are limited to a final pyrolysis temperature of 450 °C and a holding time of 60 min; they do not establish an optimum final temperature or demonstrate practical agronomic or environmental performance. Future work should examine final-temperature effects, quantify pore characteristics, and test the intended applications directly.

ACKNOWLEDGMENTS

The authors gratefully acknowledge the financial support provided by the Espírito Santo Research and Innovation Support Foundation (FAPES) through Grants No. 1254/2025 (P: 2025-3SFPC), 765/2025 (P: 2025-BP5JC), and 1672/2025 (P: 2025-N31VL); the National Council for Scientific and Technological Development (CNPq), Grant No. 448271/2025-7; and the Coordination for the Improvement of Higher Education Personnel (CAPES). The authors also acknowledge the Federal University of Espírito Santo (UFES) for the institutional support and infrastructure provided for the development of this research.

Conflict of Interest

The authors declare that they have no conflicts of interest that could have influenced the research or the publication of this manuscript.

Use of Generative AI

ChatGPT (OpenAI) was used to assist with language editing and the organization of selected passages of the manuscript. The authors reviewed and revised all AI-assisted text and take full responsibility for the content. Generative AI was not used to prepare images, figures, graphs, or diagrams.

REFERENCES CITED

ASTM D1762-84 (2021). "Standard test method for chemical analysis of wood charcoal," ASTM International, West Conshohocken, PA, USA.

Bongomin, O., Elagroudy, S., Mwasiagi, J. I., and Nzila, C. (2025). "Synergistic and antagonistic interactions in the co-pyrolysis of macadamia nutshells and coffee husks: Thermogravimetric, kinetic, and thermodynamic insights," *Bioresource Technology Reports* 31, article 102207. https://doi.org/10.1016/j.biteb.2025.102207

Carrier, M., Hugo, T., Gorgens, J., and Knoetze, H. (2011). "Comparison of slow and vacuum pyrolysis of sugar cane bagasse," *Journal of Analytical and Applied Pyrolysis* 90(1), 18-26. https://doi.org/10.1016/j.jaap.2010.10.001

Chen, D., Zhou, J., and Zhang, Q. (2014). "Effects of heating rate on slow pyrolysis behavior, kinetic parameters and products properties of moso bamboo," *Bioresource Technology* 169, 313-319. https://doi.org/10.1016/j.biortech.2014.07.009

Cheng, J., Hu, S.-C., Kang, K., Li, X.-M., Geng, Z.-C., and Zhu, M.-Q. (2021). "The effects of pyrolysis temperature and storage time on the compositions and properties of the pyroligneous acids generated from cotton stalk based on a polygeneration process," *Industrial Crops and Products* 161, article 113226. https://doi.org/10.1016/j.indcrop.2020.113226

Chmingui, W., Dridi, I., Zaier, H., Lerch, T. Z., Hammecker, C., and Hachicha, M. (2026). "Vacuum pyrolysis of olive pomace for biochar production: Enhancing carbon stability and soil nutrient supply," *Results in Engineering* 29, article 108662. https://doi.org/10.1016/j.rineng.2025.108662

Companhia Nacional de Abastecimento (CONAB) (2026). *Acompanhamento da Safra Brasileira de Café* [Monitoring of the Brazilian Coffee Crop], 13(1), Brasília, DF, Brazil.

Ding, W., Dong, X., Ime, I. M., Gao, B., and Ma, L. Q. (2014). "Pyrolytic temperatures impact lead sorption mechanisms by bagasse biochars," *Chemosphere* 105, 68-74. https://doi.org/10.1016/j.chemosphere.2013.12.042

Domingues, R. R., Trugilho, P. F., Silva, C. A., de Melo, I. C. N. A., Melo, L. C. A., Magriotis, Z. M., and Sánchez-Monedero, M. A. (2017). "Properties of biochar derived from wood and high-nutrient biomasses with the aim of agronomic and environmental benefits," *PLOS ONE* 12(5), article e0176884. https://doi.org/10.1371/journal.pone.0176884

Foong, S. Y., Liew, R. K., Yang, Y., Cheng, Y. W., Yek, P. N. Y., Wan Mahari, W. A., Lee, X. Y., Han, C. S., Vo, D.-V. N., Van Le, Q., *et al.* (2020). "Valorization of biomass waste to engineered activated biochar by microwave pyrolysis: Progress, challenges, and future directions," *Chemical Engineering Journal* 389, article 124401. https://doi.org/10.1016/j.cej.2020.124401

Guimarães, T., de Carvalho Teixeira, A. P., de Oliveira, A. F., and Lopes, R. P. (2020). "Biochars obtained from arabica coffee husks by a pyrolysis process: Characterization and application in Fe(II) removal in aqueous systems," *New Journal of Chemistry* 44(8), 3310-3322. https://doi.org/10.1039/C9NJ04144C

Hassan, M., Liu, Y., Naidu, R., Parikh, S. J., Du, J., Qi, F., and Willett, I. R. (2020). "Influences of feedstock sources and pyrolysis temperature on the properties of biochar and functionality as adsorbents: A meta-analysis," *Science of the Total Environment* 744, article 140714. https://doi.org/10.1016/j.scitotenv.2020.140714

Hughes, S. R., López-Núñez, J. C., Jones, M. A., Moser, B. R., Cox, E. J., Lindquist, M., Galindo-Leva, L. Á., Riaño-Herrera, N. M., Rodriguez-Valencia, N., Gast, F., *et al.* (2014). "Sustainable conversion of coffee and other crop wastes to biofuels and bioproducts using coupled biochemical and thermochemical processes in a multi-stage biorefinery concept," *Applied Microbiology and Biotechnology* 98(20), 8413-8431. https://doi.org/10.1007/s00253-014-5991-1

Instituto Capixaba de Pesquisa, Assistência Técnica e Extensão Rural (INCAPER) (2025). *Boletim da Conjuntura Agropecuária Capixaba* [Espírito Santo Agricultural Situation Bulletin], Vitória, ES, Brazil. https://doi.org/10.54682/bcac.v11n1

Leng, L., and Huang, H. (2018). "An overview of the effect of pyrolysis process parameters on biochar stability," *Bioresource Technology* 270, 627-642. https://doi.org/10.1016/j.biortech.2018.09.030

Liu, Z., Niu, W., Chu, H., Zhou, T., and Niu, Z. (2018). "Effect of the carbonization temperature on the properties of biochar produced from the pyrolysis of crop residues," *BioResources* 13(2), 3429-3446. https://doi.org/10.15376/biores.13.2.3429-3446

Mukherjee, A., Okolie, J. A., Tyagi, R., Dalai, A. K., and Niu, C. (2021). "Pyrolysis kinetics and activation thermodynamic parameters of exhausted coffee residue and coffee husk using thermogravimetric analysis," *The Canadian Journal of Chemical Engineering* 99(8), 1683-1695. https://doi.org/10.1002/cjce.24037

Nguyen, T. T. H., Vu, N. T., Le, H. M., and Nguyen, H. S. (2025). "Effect of pyrolysis temperature and time of Robusta coffee husk on yield and product characteristics," *Journal of the Serbian Chemical Society* 90(11), 1401-1413. https://doi.org/10.2298/JSC241002005N

Ninlaphong, P., Iamsaard, K., Kullachonphuri, S., Soilueang, P., Chromkaew, Y., Nakdee, M., Uttarotai, T., Chen, Y., and Khongdee, N. (2025). "Physicochemical characterization of coffee pulp-derived biochar and its effects on soil abiotic and

biotic properties," *Cleaner Waste Systems* 12, article 100341. https://doi.org/10.1016/j.clwas.2025.100341

Panwar, N. L., and Pawar, A. (2022). "Influence of activation conditions on the physicochemical properties of activated biochar: A review," *Biomass Conversion and Biorefinery* 12(3), 925-947. https://doi.org/10.1007/s13399-020-00870-3

Pariyar, P., Kumari, K., Jain, M. K., and Jadhao, P. S. (2020). "Evaluation of change in biochar properties derived from different feedstock and pyrolysis temperature for environmental and agricultural application," *Science of the Total Environment* 713, article 136433. https://doi.org/10.1016/j.scitotenv.2019.136433

Patra, B. R., Mukherjee, A., Nanda, S., and Dalai, A. K. (2021). "Biochar production, activation and adsorptive applications: A review," *Environmental Chemistry Letters* 19(3), 2237-2259. https://doi.org/10.1007/s10311-020-01165-9

R Core Team (2024). *R: A Language and Environment for Statistical Computing*, R Foundation for Statistical Computing, Vienna, Austria, (https://www.R-project.org/), accessed 30 September 2026.

Radojević, M., Janković, B., Stojiljković, D., Jovanović, V., Čeković, I., and Manić, N. (2021). "Improved TGA-MS measurements for evolved gas analysis (EGA) during pyrolysis process of various biomass feedstocks: Syngas energy balance determination," *Thermochimica Acta* 699, article 178912. https://doi.org/10.1016/j.tca.2021.178912

Rodriguez, J. A., Lustosa Filho, J. F., Melo, L. C. A., de Assis, I. R., and de Oliveira, T. S. (2022). "Classifying the potential of biochars from agricultural and industrial waste for the recovery of Fe and Mn mining tailings," *Journal of Analytical and Applied Pyrolysis* 161, article 105383. https://doi.org/10.1016/j.jaap.2021.105383

Ronsse, F., van Hecke, S., Dickinson, D., and Prins, W. (2013). "Production and characterization of slow pyrolysis biochar: Influence of feedstock type and pyrolysis conditions," *GCB Bioenergy* 5(2), 104-115. https://doi.org/10.1111/gcbb.12018

Saraugi, S. S., Asare, F., Gazo, R., Mohanta, T. R., Saha, P., and Routray, W. (2026). "A comprehensive characterization of tender coconut waste biochar produced through slow pyrolysis at different temperatures and heating rates," *Biomass and Bioenergy* 207, article 108728. https://doi.org/10.1016/j.biombioe.2025.108728

Setter, C., Silva, F. T. M., Assis, M. R., Ataíde, C. H., Trugilho, P. F., and Oliveira, T. J. P. (2020). "Slow pyrolysis of coffee husk briquettes: Characterization of the solid and liquid fractions," *Fuel* 261, article 116420. https://doi.org/10.1016/j.fuel.2019.116420

Shetty, R., Vidya, C. S.-N., Prakash, N. B., Lux, A., and Vaculík, M. (2021). "Aluminum toxicity in plants and its possible mitigation in acid soils by biochar: A review," *Science of the Total Environment* 765, article 142744. https://doi.org/10.1016/j.scitotenv.2020.142744

Silva, E. F., Melo, L. C. A., and de Oliveira, T. S. (2026). "Co-pyrolysis of agro-industrial waste and chemical and physical characterisation of biochars," *Biomass and Bioenergy* 208, article 108766. https://doi.org/10.1016/j.biombioe.2025.108766

Silva, W. R., Carregosa, J. C., Almeida-Couto, J. M. F., Cardozo-Filho, L., and Wisniewski Jr., A. (2022). "Management of de-oiled coffee beans biomass through pyrolysis process: Towards a circular bioeconomy," *Journal of Analytical and Applied Pyrolysis* 168, article 105763. https://doi.org/10.1016/j.jaap.2022.105763

Song, Y., Tan, J., Jin, M., Liu, Z., Zhu, J., El-sayed, M. E. A., Abdelhafeez, I. A., Zhang, Y., and Shen, Z. (2025). "Effect of pyrolysis temperature and heating rate on the physicochemical properties of alkali lignin-derived biochar: A comparative study of

fast and slow pyrolysis," *Journal of Analytical and Applied Pyrolysis* 191, article 107236. https://doi.org/10.1016/j.jaap.2025.107236

Tomczyk, A., Sokołowska, Z., and Boguta, P. (2020). "Biochar physicochemical properties: Pyrolysis temperature and feedstock kind effects," *Reviews in Environmental Science and Bio/Technology* 19(1), 191-215. https://doi.org/10.1007/s11157-020-09523-3

Ullah, H., Abbas, Q., Ali, M. U., Amina, Cheema, A. I., Yousaf, B., and Rinklebe, J. (2019). "Synergistic effects of low-/medium-vacuum carbonization on physico-chemical properties and stability characteristics of biochars," *Chemical Engineering Journal* 373, 44-57. https://doi.org/10.1016/j.cej.2019.05.025

Yuan, J.-H., Xu, R.-K., and Zhang, H. (2011). "The forms of alkalis in the biochar produced from crop residues at different temperatures," *Bioresource Technology* 102(3), 3488-3497. https://doi.org/10.1016/j.biortech.2010.11.018

Zhao, B., O'Connor, D., Zhang, J., Peng, T., Shen, Z., Tsang, D. C. W., and Hou, D. (2018). "Effect of pyrolysis temperature, heating rate, and residence time on rapeseed stem derived biochar," *Journal of Cleaner Production* 174, 977-987. https://doi.org/10.1016/j.jclepro.2017.11.013

Article submitted: October 1, 2026; Peer review completed: October 31, 2026; Revised version received: November 6, 2026; Accepted: November 11, 2026; Published: November 18, 2026.
DOI: 10.15376/biores.22.1.535-557